

**NASA TECHNICAL
MEMORANDUM**



NASA TM X-3498

NASA TM X-3498

(X-3498-TM-X-3498) COLD AIR INVESTIGATION OF
4 1/2-STAGE TURBINE WITH STAGE LOADING
FACTOR OF 4.66 AND HIGH SPECIFIC WORK
OUTPUT. I: OVERALL PERFORMANCE (NASA)
C. F. MOORE, JR. AL1

577-1.1

CSCL 41c H1/17 1717c



**COLD-AIR INVESTIGATION OF 4 1/2-STAGE
TURBINE WITH STAGE LOADING FACTOR
OF 4.66 AND HIGH SPECIFIC WORK OUTPUT**

I - Overall Performance

*Warren J. Whitney, Frank P. Behning,
Thomas P. Moffitt, and Glen M. Hotz
Lewis Research Center
Cleveland, Ohio 44135*

50 N.O.P.O.

1 Report No NASA TM X-3498	2 Government Accession No	3 Recipient's Catalog No	
4 Title and Subtitle COLD-AIR INVESTIGATION OF 4½-STAGE TURBINE WITH STAGE LOADING FACTOR OF 4.66 AND HIGH SPECIFIC WORK OUTPUT I - OVERALL PERFORMANCE		5 Report Date February 1977	
		6 Performing Organization Code	
7 Author(s) Warren J. Whitney, Frank P. Behning, Thomas P. Moffitt, and Glen M. Hotz		8 Performing Organization Report No E-8967	
		10 Work Unit No	
9 Performing Organization Name and Address Lewis Research Center National Aeronautics and Space Administration Cleveland, Ohio 44135		11 Contract or Grant No	
		13 Type of Report and Period Covered Technical Memorandum	
12 Sponsoring Agency Name and Address National Aeronautics and Space Administration Washington, D.C. 20546		14 Sponsoring Agency Code	
15 Supplementary Notes			
16 Abstract <p>The turbine developed design specific work output at design speed at a total-pressure ratio of 6.745 with a corresponding efficiency of 0.855. The efficiency (0.855) was 3.1 points lower than the estimated efficiency quoted by the contractor in the design report and 0.7 of a point lower than that determined by a reference prediction method. The performance of the turbine, which was a forced vortex design, agreed with the performance determined by the prediction method to about the same extent as did the performance of three reference high-stage-loading-factor turbines, which were free vortex designs.</p>			
17 Key Words (Suggested by Author(s)) Turbine aerodynamics High stage loading		18 Distribution Statement Unclassified - unlimited STAR Category 07	
19 Security Classif. (of this report) Unclassified	20 Security Classif. (of this page) Unclassified	21 No. of Pages 20	22 Price* A02

COLD-AIR INVESTIGATION OF $4\frac{1}{2}$ -STAGE TURBINE WITH STAGE LOADING

FACTOR OF 4.66 AND HIGH SPECIFIC WORK OUTPUT

1 - OVERALL PERFORMANCE

by Warren J. Whitney, Frank P. Behning, Thomas P. Moffitt, and Glen M. Hotz

Lewis Research Center

SUMMARY

The overall performance of a $4\frac{1}{2}$ -stage turbine with a stage loading factor of 4.66 and high specific work output was determined in cold air. The turbine developed design specific work output at design speed at a total-pressure ratio of 6.745 with a corresponding efficiency of 0.855. The mass flow at this condition was 6.033 kilograms per second (13.3 lb/sec), or 0.992 of design mass flow. The efficiency (0.855) was 3.1 points lower than the estimated efficiency (0.886) quoted by the contractor in the design report and 0.7 of a point lower than that determined by a reference prediction method. The performance of the turbine, which was a forced vortex design, agreed with the performance determined by the prediction method to about the same extent as did the performance of three reference high-stage-loading-factor turbines, which were free vortex designs. In all cases the predicted efficiency was within 0.01 of the experimental value. The estimated design point efficiency of 0.886 was not achieved at any Reynolds number investigated, including the design value.

INTRODUCTION

In the past few years the NASA Lewis Research Center has devoted research effort to turbines designed to operate with high stage loading factor (e. g., refs. 1 to 3). The turbine of reference 1 was the fan drive turbine of a study engine for a VSTOL aircraft. This turbine had $3\frac{1}{2}$ stages and an average stage loading factor (ratio of change in tangential velocity to blade speed) of 4. The $4\frac{1}{2}$ -stage turbine of reference 2 had an average stage loading factor of 5, and the three-stage turbine of reference 3 had an average

stage loading factor of 3.

These high-stage-loading-factor turbines are typified by low blade speed, shrouded rotor blades, and a large amount of turning in both the stator blade row and the rotor blade row. The alternative to using high stage loading is using conventional loading factors (2 or lower), and thereby doubling or tripling the number of stages, or driving the fan through a gearbox.

In the work of reference 1 the efficiency of high-stage-loading-factor turbines was predicted by using the stage efficiencies from reference 4 and, where applicable, the outlet turning vane loss determined from reference 5. The predicted efficiencies were within 1 point of the experimental efficiencies for all three turbines, and this order of agreement demonstrated the adequacy of the prediction method.

The subject turbine evolved from a study made by Pratt & Whitney Aircraft (P&WA) of East Hartford, Connecticut, of the engine needs for a future or advanced transport airplane. The turbine was designed by P&WA to drive the fan of the engine. The design procedure is discussed in reference 6. The turbine had four stages with outlet turning vanes and employed an average stage loading factor of 4.66. The specific work requirement was 1.73 times that of the reference 2 turbine, and this increased work output represented an added degree of design difficulty as compared with that of the reference turbine. An efficiency of 0.886 was anticipated for this turbine by the contractor in reference 6. This efficiency is 2.4 points higher than that which would have been predicted by using the prediction method based on references 4 and 5. The pertinent features of the design which the contractor contended would result in good performance were (1) controlled or forced vortex flow with a tailored radial work distribution and (2) controlled position of the boundary-layer transition point on the airfoil suction surface to result in minimum profile loss. It was, therefore, of interest to determine the turbine performance and experimentally verify the merit of these design features.

The turbine aerodynamic and mechanical designs were conducted by P&WA and are discussed in reference 6. A one-half-scale model of the engine turbine was fabricated under P&WA supervision. The model turbine (mean diameter, 0.48006 m) was then sent to the Lewis Research Center for performance evaluation.

This report presents the results of the performance investigation. The turbine performance was obtained with inlet total pressure and total temperature maintained at 2.4 atmospheres and 444 K (800° R), respectively. The turbine was operated at speeds of 70 to 120 percent of design speed, and total-pressure ratio was varied over a wide range (bracketing design pressure ratio) at each speed. In addition to the general performance tests, a limited number of test points were obtained to investigate Reynolds number effect. These points were obtained by varying inlet pressure at design speed, design work output, and constant inlet temperature.

SYMBOLS

A	area, m^2 ; ft^2
\bar{D}_m	effective mean diameter, $\sqrt{\frac{D_{m,1}^2 + D_{m,2}^2 + D_{m,3}^2 + D_{m,4}^2}{4}}$, m; ft
$\left. \begin{matrix} D_{m,1}, D_{m,2} \\ D_{m,3}, D_{m,4} \end{matrix} \right\}$	mean diameters of first, second, third, and fourth stages, respectively
g	force-mass conversion constant, 1; 32.174 ft/sec^2
h	specific enthalpy, J/g; Btu/lb
N	rotative speed, rpm
n	number of stages
P	absolute pressure, N/m^2 ; lb/ft^2
R	gas constant for mixture of air and combustion products used in this investigation, 287.9 J/(kg)(K); 53.463 (ft-lb)/(lb)(°R)
RI	Reynolds number index based on turbine inlet conditions, $P_0/\mu_0 V_{cr,0}$, 1/m; 1/ft
T	temperature, K; °R
U	blade velocity, m/sec; ft/sec
\bar{U}_m	effective mean blade speed, $(\pi \bar{D}_m N)/60$ m/sec; ft/sec
V	absolute gas velocity, m/sec; ft/sec
W	gas velocity relative to moving blade, m/sec; ft/sec
w	mass flow rate (sum of air and fuel), kg/sec; lb/sec
α	absolute gas flow angle measured from axial direction, deg
$\bar{\alpha}$	average absolute gas flow angle at turbine outlet measured from axial direction irrespective of sign, used in eq. (2), deg
β	angle of gas flow relative to moving blade measured from axial direction, deg
γ	ratio of specific heats, 1.3949 for mixture of air and combustion products used in this investigation
δ	ratio of inlet pressure to U.S. standard sea-level pressure

ϵ	function of γ , $(0.73959/\gamma)[(\gamma + 1)/2]^{\gamma/(\gamma-1)}$
η	efficiency based on total-pressure ratio
θ_{cr}	squared ratio of critical velocity at turbine inlet to critical velocity of U.S. standard sea-level air
μ	viscosity, (N)(sec)/m ² ; (lb)(sec)/ft ²
τ	torque, N-m; ft-lb

Subscripts:

cr	condition at Mach 1
0	station at turbine inlet (see fig. 3)
0.5, 1.0, 1.5, 2.0, } 2.5, 3.0, 3.5, 4.0 }	interstage cavity pressure tap stations (see fig. 3)
4.5	station at turbine outlet (see fig. 3)

Superscript:

'	total state
---	-------------

TURBINE DESCRIPTION

As mentioned in the INTRODUCTION, the turbine evolved from a study of the engine for an advanced transport airplane. The turbine described in reference 6 and in this report is a one-half-scale model of the engine fan drive turbine. The subject turbine design requirements and physical characteristics are as follows:

Number of stages, n	4
Average stage loading factor, $\Delta h \times 10^3 / (n \times \bar{U}_m^2)$	4.66
Equivalent specific work, $\Delta h / \theta_{cr}$, J/g; Btu/lb	104.44; 44.9
Equivalent mass flow, $\epsilon w \sqrt{\theta_{cr}} / \delta$, kg/sec; lb/sec	6.078; 13.4
Equivalent effective mean blade speed, \bar{U}_m , m/sec; ft/sec	74.905; 245.75
Effective mean diameter, \bar{D}_m , m; ft	0.48006; 1.575
Equivalent rotative speed, $N / \sqrt{\theta_{cr}}$, rpm	2980
Total-pressure ratio, $P_0 / P_{4.5}$, based on estimated efficiency of 0.886	6.18

The turbine design incorporated forced vortex flow with the specific work extraction varied along the radius (ref. 6). The contractor contended that this type of design has an advantage over free vortex flow in that the reaction is more favorable at both the hub and the tip sections. The contractor also maintained that improved performance would result from controlling the location of the transition point of the airfoil suction surface boundary layer. The argument was that a minimum profile loss results when this transition point occurs just before the suction surface minimum pressure point. Since the boundary-layer flow phenomena are dependent on Reynolds number, the following turbine inlet conditions corresponding to design Reynolds number were given by the contractor: inlet pressure, 1.565 atmospheres; inlet temperature, 422 K (760° R).

The layout of the blade passages and the mechanical design of the turbine are described in reference 6. The velocity diagrams from reference 6 for the hub, mean, and tip sections are shown in figure 1. The blading passages and profiles are shown in figure 2. The flow path through the turbine and the instrumentation stations are depicted in figure 3. The mean diameter and tip diameter increase from inlet to outlet, and the hub diameter decreases slightly. The effective mean diameter was, therefore, defined as the root-mean-square value. The turbine rotor assembly is shown in figure 4.

APPARATUS, INSTRUMENTATION, AND PROCEDURE

The test facility is the same as that used in the work of reference 1 and described in reference 7. The turbine installed in the facility is shown in figure 5. The type of research data and the data acquisition system are nearly the same as those described in reference 7. Turbine airflow was measured with a calibrated Dall tube, which is a modified form of venturi meter. The fuel flow to the turbine inlet-air heater was metered with a flat-plate orifice. Both of these flow measurements required an upstream temperature, an upstream pressure, and a characteristic differential pressure. The turbine mass flow was obtained as the sum of the fuel flow and airflow.

Turbine rotative speed was measured with a magnetic pickup mounted close to the periphery of a square-tooth sprocket which was fixed to the turbine shaft. An electronic counter registered the impulses from the pickup and converted this signal to rotative speed. The turbine output torque was determined by measuring the reaction torque on the cradled dynamometer stator with a strain-gage load cell. The load cell and the digital voltmeter readout system were calibrated before and after each day's running.

The turbine was instrumented at the stations indicated in figure 3. The instrumentation at the turbine inlet, station 0, and the turbine outlet, station 4.5, is represented by the sketches in figure 6. At the turbine inlet, station 0, the instrumentation con-

sisted of eight wall static-pressure taps (four inner and four outer), nine bare-wire spike thermocouples (three rakes of three each), and two Kiel total-pressure probes. The inlet thermocouples were located at the area center radii of three equal annular areas. The thermocouples were corrected for recovery coefficient and were averaged to obtain turbine inlet total temperature T'_0 .

At the turbine outlet, station 4.5, the instrumentation consisted of eight wall static-pressure taps (four inner and four outer), two five-element total-temperature rakes, and three combination angle and total-pressure probes (fig. 6). The thermocouple elements were located at the area center radii of five equal annular areas. Each of the three combination probes was traversed in steps across the radial span, and angle and total-pressure readings were taken at the area center radii of five equal annular areas. The static pressure and flow angle at the turbine outlet were used in the efficiency calculation. The indicated total pressure and total temperature were obtained to provide a rough check of the calculated total pressure and total temperature.

At the interstage stations (0.5, 1.0, 1.5, 2.0, 2.5, 3.0, 3.5, and 4.0) static pressures were measured (three each at each station) in the outer clearance space. These interstage cavity pressures were taken for comparison with those to be obtained in follow-on tests of the three-, two-, and one-stage configurations to determine the stage work distribution.

The inlet total pressure was calculated from the static pressure, mass flow rate, annular area, and inlet total temperature by using the following equation:

$$\frac{P'_0}{P_0} = \left[\frac{1}{2} + \sqrt{\frac{1}{4} + \frac{\gamma - 1}{2g\gamma} \left(\frac{w}{P_0 A_0} \right)^2 RT'_0} \right]^{\gamma/(\gamma-1)} \quad (1)$$

The outlet total pressure was calculated in a similar manner; however, since the flow is not axial, the flow angle must be included in the equation:

$$\frac{P'_{4.5}}{P_{4.5}} = \left[\frac{1}{2} + \sqrt{\frac{1}{4} + \frac{\gamma - 1}{2g\gamma} \left(\frac{w}{P_{4.5} A_{4.5}} \right)^2 \frac{RT'_{4.5}}{\cos^2 \bar{\alpha}}} \right]^{\gamma/(\gamma-1)} \quad (2)$$

The total temperature $T'_{4.5}$ in equation (2) was calculated from the inlet temperature T'_0 , turbine speed, torque, and mass flow. The angle $\bar{\alpha}$ in equation (2) is the average deviation from the axial direction, irrespective of sign.

The data were obtained for nominal inlet conditions of 2.4 atmospheres and 444 K (800° R). The turbine was investigated at speeds of 70, 80, 90, 100, 110, and 120 percent of design equivalent speed. At each speed the total-pressure ratio was varied over a wide range bracketing design pressure ratio. In addition, a limited number of points were obtained to investigate Reynolds number effect by varying inlet pressure at design speed, design work output, and constant inlet temperature.

RESULTS AND DISCUSSION

Overall Performance

The experimental data are presented in figures 7 and 8 with equivalent mass flow $\epsilon w \sqrt{\theta_{cr}}/\delta$ and equivalent torque $\epsilon \tau/\delta$ shown as functions of the turbine total-pressure ratio $P'_0/P'_{4.5}$. Most of the data fall close to the faired curves. Although figure 7 shows some scatter in the mass flow, it should be noted that the ordinate scale is magnified, and the greatest deviation from the curve is 0.4 of 1 percent. The turbine choked at all speeds (fig. 7) with the choking pressure ratio varying from 4.0 at 70 percent of design speed to 7.0 at 120 percent of design speed. Figure 8 indicates that the turbine did not reach limiting loading at any speed for the range of pressure ratios covered.

The experimental data of figures 7 and 8 were combined to construct the overall performance map (fig. 9). The efficiency obtained at design specific work output and design speed was 0.855. This is 0.031 lower than the efficiency value anticipated by the contractor in reference 6. The mass flow at this condition was 8.033 kilograms per second (13.3 lb/sec), or 0.992 of design mass flow, and the pressure ratio $P'_0/P'_{4.5}$ was 6.745. The highest efficiency obtained was 0.88, which occurred at 120 percent of design speed at pressure ratios from 5 to 7 (average stage loading factor, 2.9 to 3.4).

Efficiency Comparison

As mentioned in the preceding section, the experimentally obtained efficiency at design equivalent work extraction and design speed was 0.855, which was 3 points lower than the estimated efficiency of 0.886 quoted in the design report (ref. 6). It was, therefore, of interest to determine a predicted efficiency by using the stage efficiencies from reference 4 and the outlet turning vane loss from reference 5. The resulting predicted efficiency for the 4½-stage turbine was 0.862, or 0.007 higher than

the experimental value. This result agreed closely with that obtained in reference 1, although the Reynolds number was higher than that of the reference 1 tests. Table I compares the experimental efficiency with the predicted efficiency for the subject turbine and the three reference turbines. In all cases the predicted efficiency was within 0.01 of the experimental value. This agreement substantiates the adequacy of the prediction procedure for high-stage-loading-factor turbines. It might also be noted that the agreement between predicted performance and experimental performance for the subject turbine, which was a forced vortex design, was about the same as that obtained for the three reference turbines, which were free vortex designs.

Effect of Reynolds Number on Performance

As mentioned previously, the data were obtained for an inlet pressure and temperature of 2.4 atmospheres and 444 K (800° R), respectively. The pressure was selected to obtain the highest accuracy within the limits of the test facility. It was also felt to be important to determine the turbine performance at design Reynolds number, since the control of the suction surface boundary-layer transition point was purported by P&WA to be an important feature of the design, and the boundary-layer flow phenomena are dependent on Reynolds number. A number of test points were, therefore, obtained at reduced inlet pressure to include design Reynolds number, which is defined in reference 6 by the inlet conditions of 1.565 atmospheres and 422 K (760° R).

The results of these tests are shown in figure 10. The efficiency decreased from 0.855 at the normal test conditions to 0.848 at design Reynolds number. This decrease in efficiency with decreasing Reynolds number was also noted for the turbines of references 2 and 3.

In summary, the turbine performance agreed with the performance predicted by using references 4 and 5 to about the same extent as that of the reference turbines, which were free vortex designs. Thus, the design efficiency estimate of 0.886, or 2.4 points higher than the predicted efficiency, was not achieved at design work output and design speed for any Reynolds number investigated, including the design value.

SUMMARY OF RESULTS

A $4\frac{1}{2}$ -stage turbine with a stage loading factor of 4.66 and high specific work output was investigated experimentally in cold air. The following results were obtained:

1. The turbine developed design specific work output at design speed with an efficiency of 0.855. The mass flow at this condition was 6.033 kilograms per second (13.3 lb/sec), or 0.992 of design mass flow, and the pressure ratio was 6.745.

2. The efficiency at design specific work output and design speed was 0.031 lower than the efficiency anticipated in the design report. The efficiency predicted for this turbine by a reference prediction method was 0.862, or 0.007 higher than the experimental value.

3. The experimentally obtained efficiencies of this turbine and three reference high-stage-loading-factor turbines were compared with the efficiencies obtained from a reference prediction method. In all cases the predicted efficiency was within 0.01 of the experimental value.

4. The design efficiency estimate of 0.886, which was 2.4 points higher than the predicted efficiency, was not achieved at design speed and design work output for any Reynolds number investigated, including the design value.

Lewis Research Center,
National Aeronautics and Space Administration,
Cleveland, Ohio, November 9, 1976,
505-04.

REFERENCES

1. Whitney, Warren J.; Schum, Harold J.; and Behning, Frank P.: Cold-Air Investigation of a $3\frac{1}{2}$ Stage Fan-Drive Turbine With a Stage Loading Factor of 4 Designed for an Integral Lift Engine. II - Performance of 2-Stage, 3-Stage, and $3\frac{1}{2}$ -Stage Configurations. NASA TM X-3482, 1977.
2. Walker, N. D.; and Thomas, M. W.: Experimental Investigation of a $4\frac{1}{2}$ -Stage Turbine With Very High Stage Loading Factor. II - Turbine Performance. NASA CR-2363, 1974.
3. Wolfmeyer, G. W.; and Thomas, M. W.: Highly Loaded Multi-Stage Fan Drive Turbine - Performance of Initial Seven Configurations. NASA CR-2362, 1974.
4. Stewart, Warner L.; and Glassman, Arthur J.: Analysis of Fan-Turbine Efficiency Characteristics in Terms of Size and Stage Number. NASA TM X-1581, 1968.
5. Aerodynamic Design of Axial Flow Compressors. Revised, NASA SP-36, 1965.
6. Webster, P. F.: Design of a $4\frac{1}{2}$ -Stage Turbine With a Stage Loading Factor of 4.66 and High Specific Work Output. NASA CR-2659, 1976.
7. Whitney, Warren J.; Schum, Harold J.; and Behning, Frank P.: Cold-Air Investigation of a Turbine for High-Temperature-Engine Application. IV - Two-Stage Turbine Performance. NASA TN D-6960, 1972.

TABLE I. - COMPARISON OF EXPERIMENTAL AND PREDICTED
EFFICIENCIES OF HIGH-STAGE-LOADING-1 ACTOR TURBINES

Number of turbine stages	Reference	Average stage loading factor	Efficiency predicted by using refs. 4 and 5	Experimental efficiency	Reynolds number index, $RI, 1/m$
$3\frac{1}{2}$	1	4	0.863	0.855	1.72×10^7
3	3	3	0.891	0.886 .882	2.55×10^7 1.70
$4\frac{1}{2}$	2	5	0.843	0.852 .847	3.29×10^7 2.06
$4\frac{1}{2}$	This report	4.66	0.862	0.855 .848	2.53×10^7 1.73

Figure 1 - velocity diagrams. Numbers are angles in degrees and slash numbers at airfoil exit. (from ref. 9)

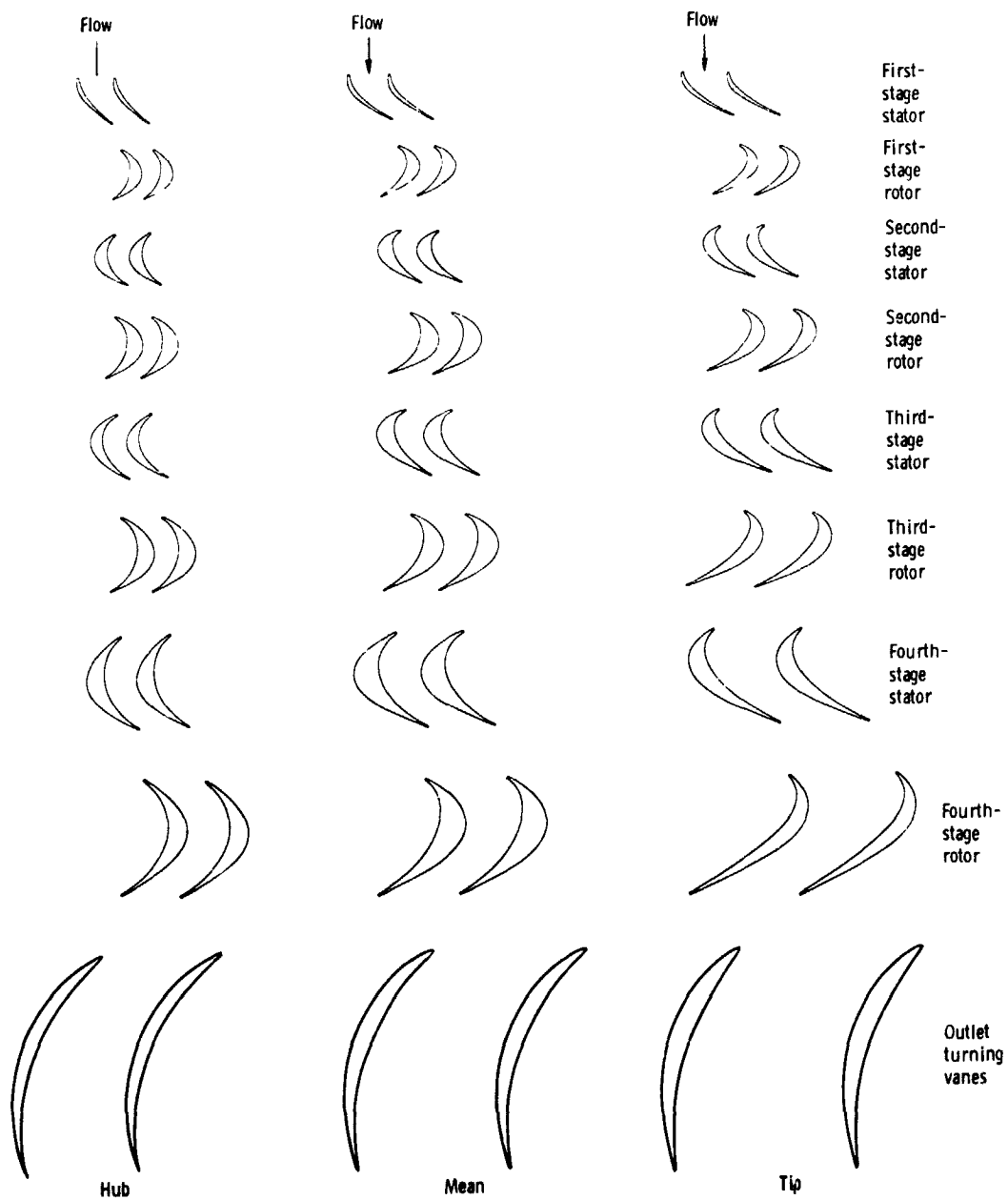


Figure 2. - Turbine blading passages and profiles.

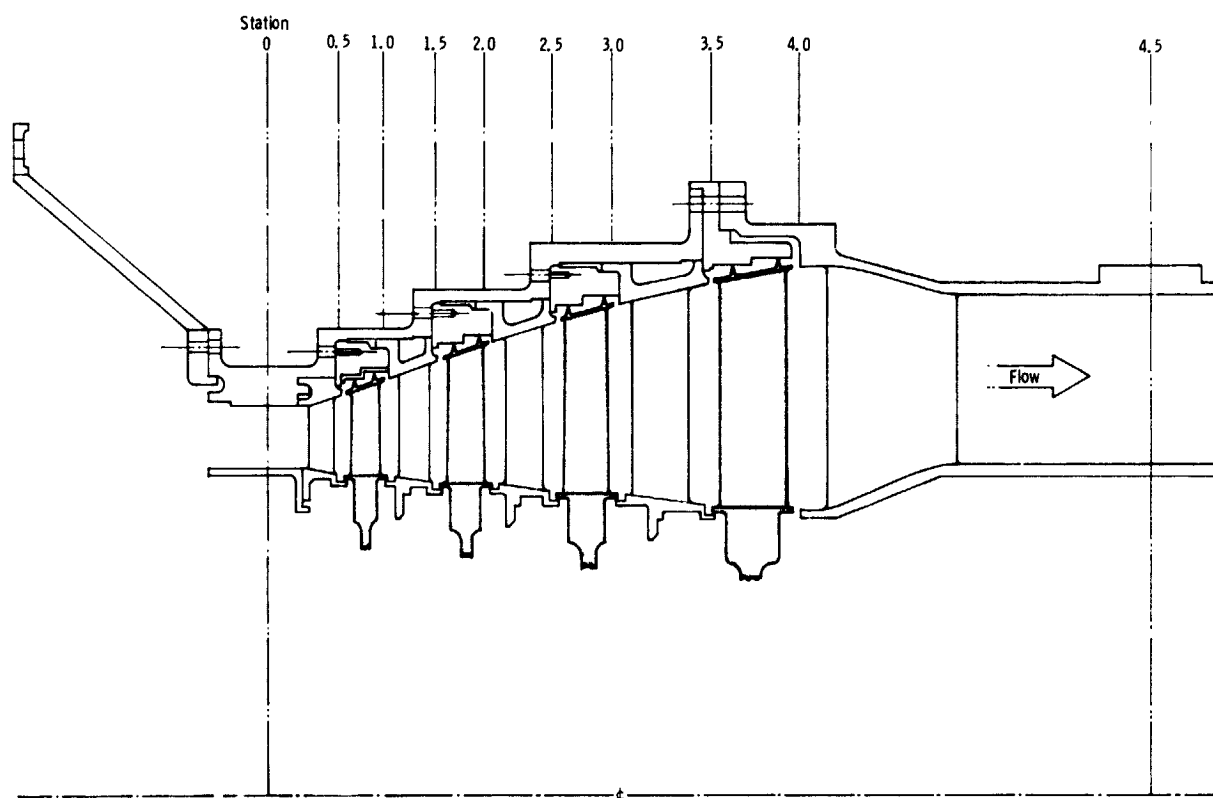


Figure 3. - Flow path and instrumentation stations.

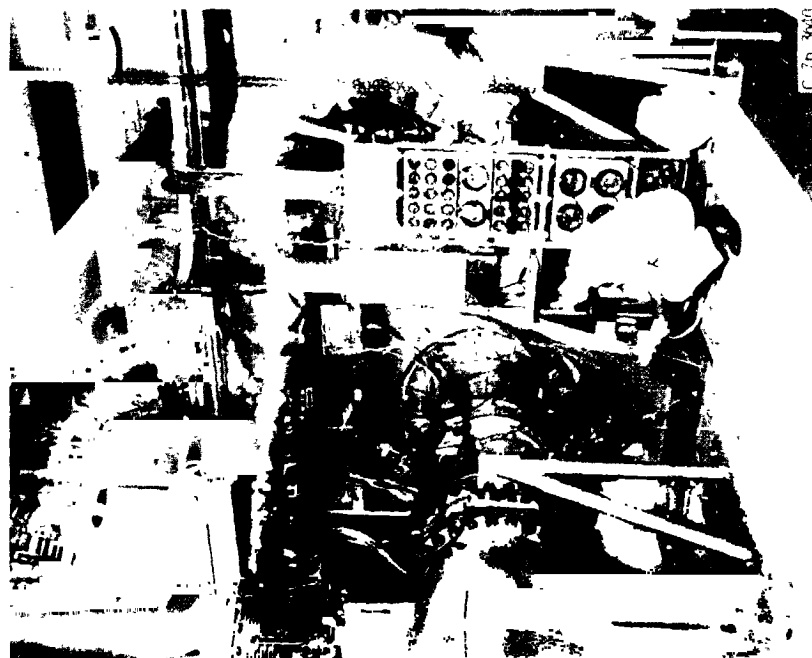


Figure 5. - Turbine installed in test facility.

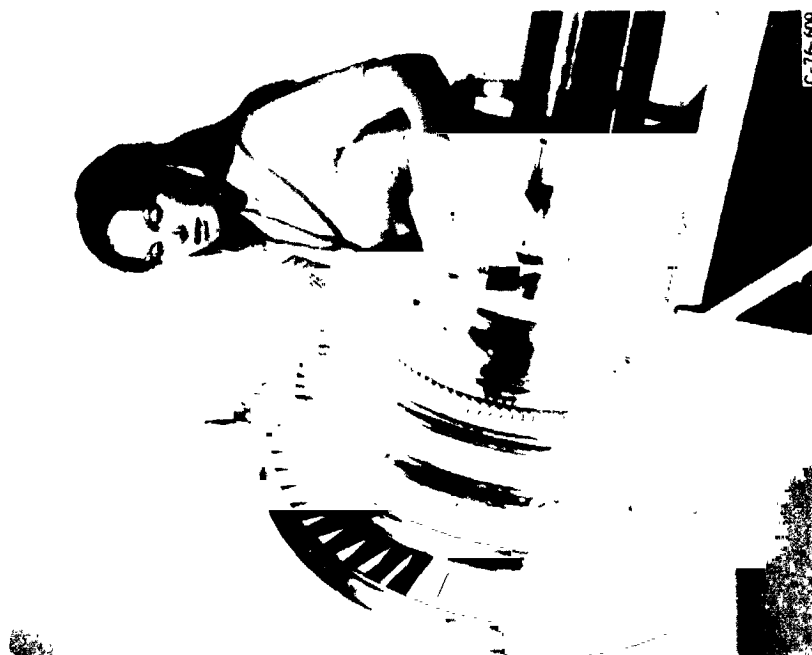
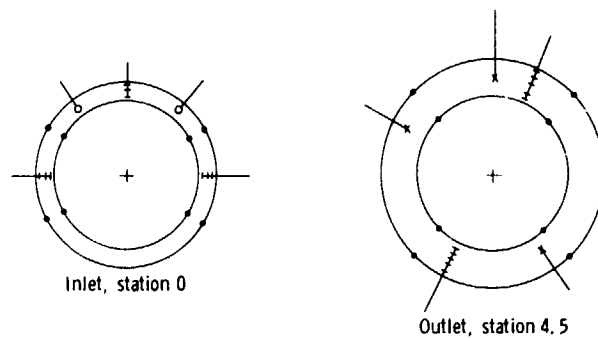


Figure 4. - Turbine rotor assembly.



- Wall static tap
- Thermocouple rake
- Kiel total-pressure probe
- ✱ Combination angle and total-pressure probe

Figure 6. - Instrumentation plan.

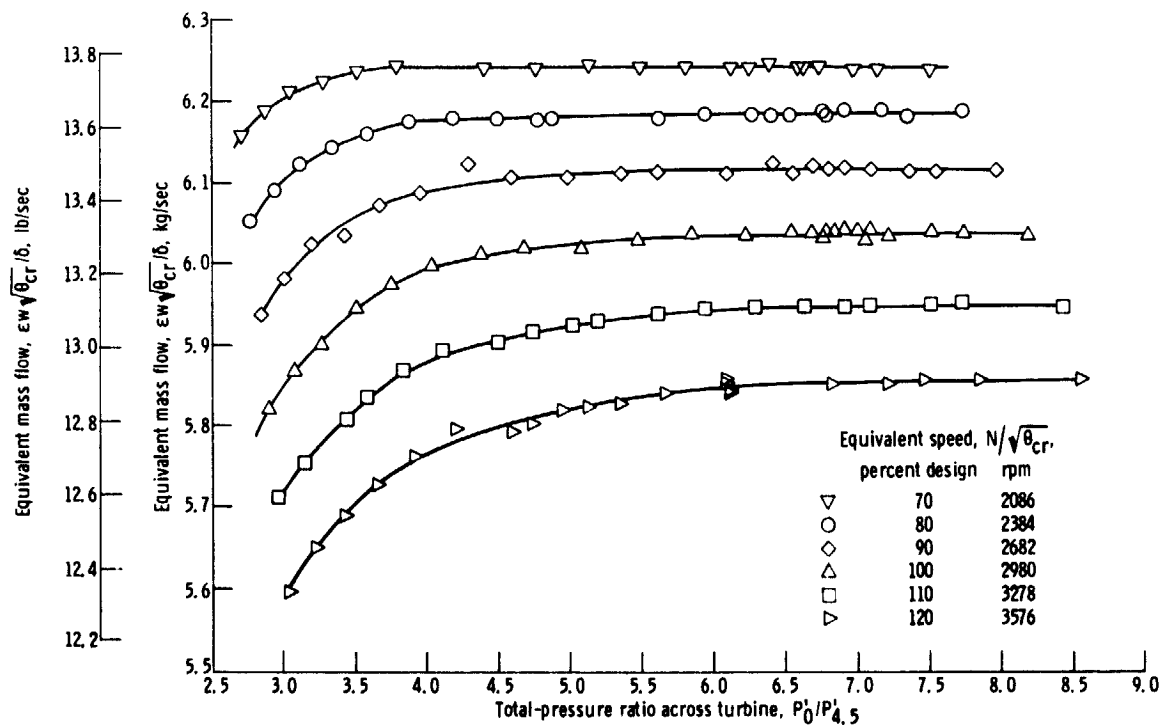


Figure 7. - Variation of equivalent mass flow with total-pressure ratio for various speeds.

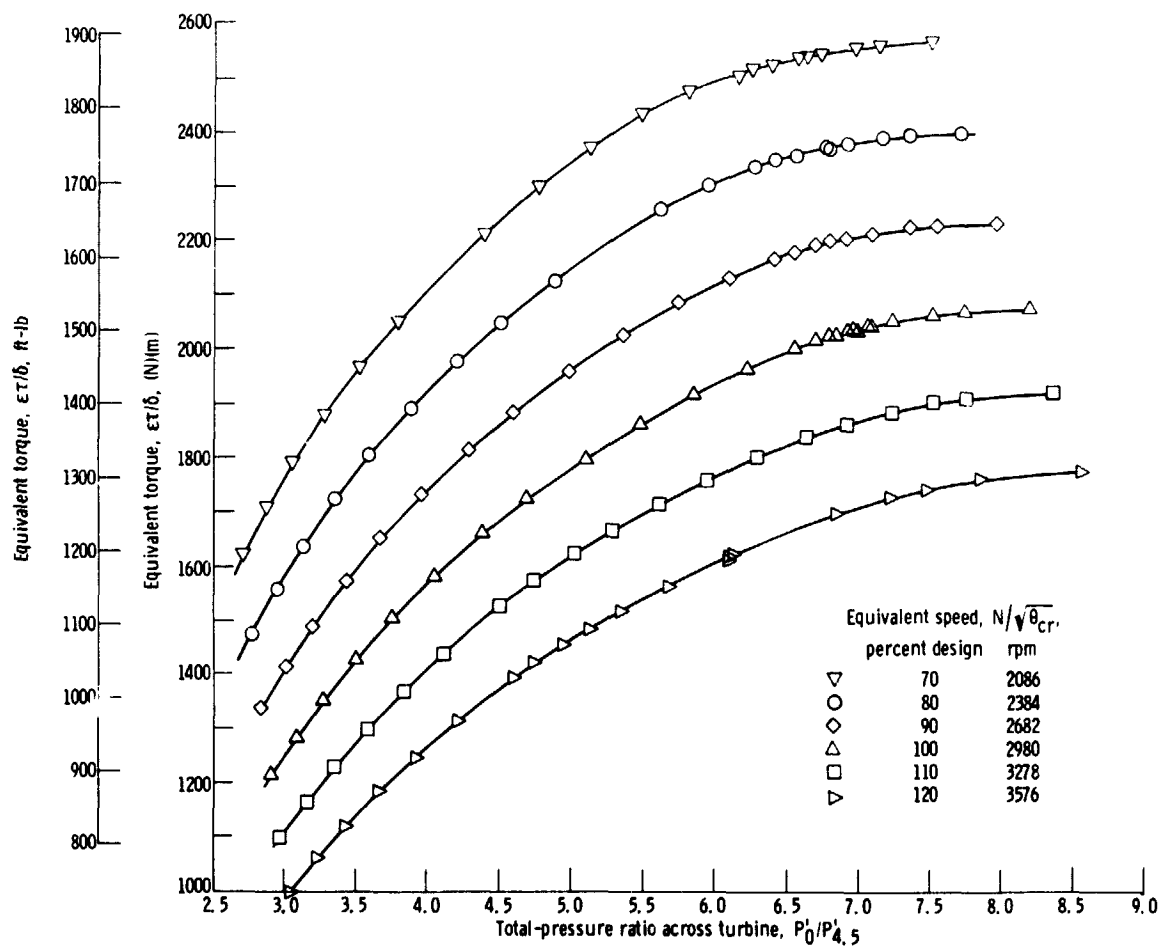


Figure 8. - Variation of equivalent torque with total-pressure ratio for various speeds.

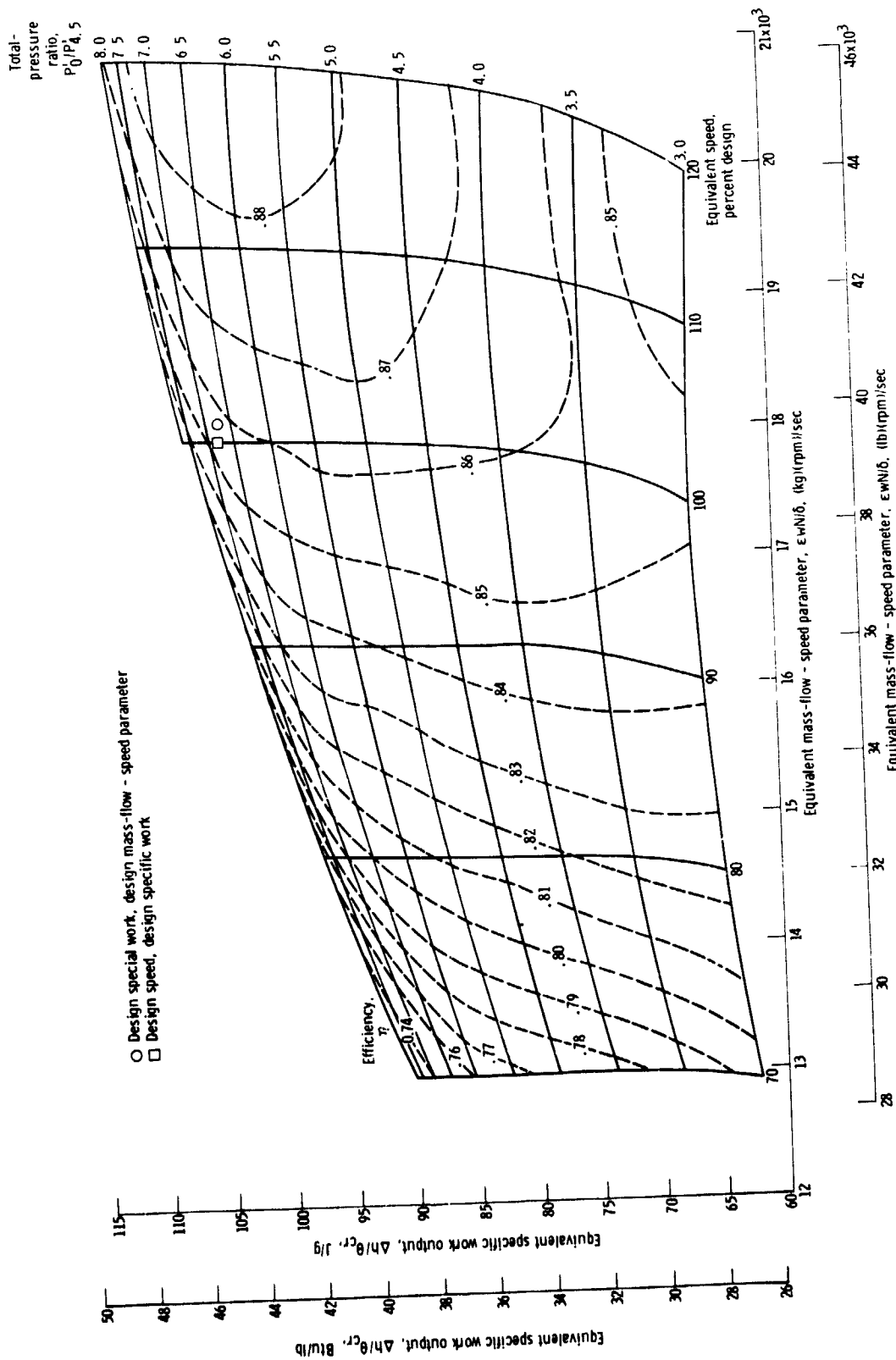


Figure 9. - Performance map.

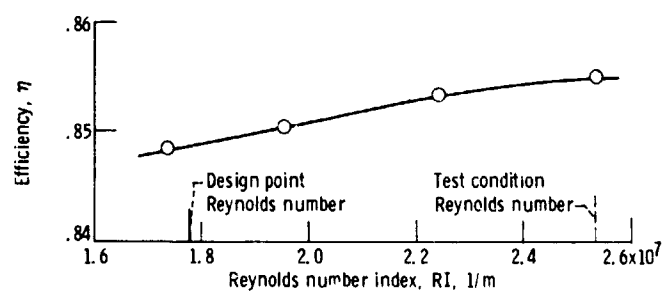


Figure 10. - Effect of Reynolds number on overall performance at equivalent design speed, equivalent design work extraction, and constant inlet temperature.